Research Article

Modeling protein-protein interactions in axon initial segment to understand their potential impact on action potential initiation

https://doi.org/10.4103/1673-5374.295332

Received: November 26, 2019

Peer review started: December 2, 2019

Accepted: May 20, 2020

Published online: October 9, 2020

Piyush Bhardwaj[1, 2], Don Kulasiri[1, 2, *], Sandhya Samarasinghe[1]

Abstract

The axon initial segment (AIS) region is crucial for action potential initiation due to the presence of high-density AIS protein voltage-gated sodium channels (Na_v). Na_v channels comprise several serine residues responsible for the recruitment of Na_v channels into the structure of AIS through interactions with ankyrin-G (AnkG). In this study, a series of computational experiments are performed to understand the role of AIS proteins casein kinase 2 and AnkG on Na_v channel recruitment into the AIS. The computational simulation results using Virtual cell software indicate that Na_v channels with all serine sites available for phosphorylation bind to AnkG with strong affinity. At the low initial concentration of AnkG and casein kinase 2, the concentration of Na_v channels reduces significantly, suggesting the importance of casein kinase 2 and AnkG in the recruitment of Na_v channels.

Key Words: Alzheimer's disease; ankyrin-G; axon initial segment; casein kinase-2; microtubules; voltage-gated potassium channel; voltage-gated sodium channel

Chinese Library Classification No. R448; R31; R741

Introduction

Communication between neurons through action potentials (AP) is necessary for the nervous system to perform its functions. An AP is characterized by the changes in membrane potential or membrane voltage due to the efflux and influx of cations. Several studies have confirmed that AP is initiated at the axon initial segment (AIS) (Lemaillet et al., 2003; Rasband, 2009; Kole and Stuart, 2012; Gulledge and Bravo, 2016), which is a non-myelinated region (**Figure 1**), with a length of 10 to 60 µm, at the beginning of an axon (Kole et al., 2008; Buffington and Rasband, 2011; Kole and Stuart, 2012; Leterrier et al., 2015; Jones and Svitkina, 2016; Nelson and Jenkins, 2017; Fan and Markram, 2019). The main proteins in the AIS are voltage-gated sodium channels (Na_v), voltage-gated potassium channels (K_v), microtubules (MTs), casein kinase 2 (CK2), and ankyrin-G (AnkG). AnkG is an essential protein in the AIS because the recruitment of other proteins (K_v, Na_v, neurofascin 186 [NF186], and neuronal cell adhesion molecule [NrCAM]) into the AIS depends on it (Hedstrom et al., 2008; Jones and Svitkina, 2016). To evaluate the importance of AIS in neurological processes and to show its relationships with various neurological diseases, it is necessary to understand the structural organization of the AIS region (**Figure 1**).

CK2, a serine/threonine-specific kinase, is acidophilic in nature and mediates phosphorylation of various proteins in the AIS (Meggio and Pinna, 2003). CK2 is constitutively active and does not require any second messenger or phosphorylation event to be activated (Meggio and Pinna, 2003; Bian et al., 2013). During the developmental stage, the early presence of CK2 in neurons has been observed, even before axon formation, and the experiments have shown the shortening of axons by 30% after CK2 inhibition (Ponce et al., 2011). CK2 plays a very critical role in AnkG-Na_v binding to recruit Na_v channels into the AIS facilitating the phosphorylation of Na_v channels to increase their affinity towards AnkG (Rasband, 2008; Yamada and Kuba, 2016). Na_v channels comprise a special type of amino acid sequence called the AIS motif, where the binding with AnkG takes place. The AIS motif contains four serine residues at different positions, S1112, S1123, S1124, and S1126 (**Figure 2**; Schafer et al., 2009). In addition to that, the AIS motif also contains the acidic residues: glutamate (E) and aspartate (D) residues are present at 1111 and 1113 positions respectively (**Figure 2**). All these residues have different functions in the AIS motif: the serine residues are responsible for the phosphorylation of Na_v channels through CK2, and acidic residues (glutamate and aspartate) increase the affinity of phosphorylation process (Meggio and Pinna, 2003). All these serine sites are phosphorylated by CK2 and this increases the binding affinity of the Na_v channels towards AnkG to restrict them at the AIS (Meggio and Pinna, 2003; Brechet et al., 2008; Bian et al., 2013).

Any alteration in neuronal transmission can cause various neurological conditions, such as Alzheimer's disease (AD), epilepsy, schizophrenia and bipolar disorder (Buffington and Rasband, 2011; Kaphzan et al., 2011; Bi et al., 2012; Harty et al., 2013; Rueckert et al., 2013; Peltola et al., 2016). AD is the most common neurodegenerative disease in humans; thus, it is the most common cause of dementia and, as yet, there is no known cure for AD (Hardy and Higgins, 1992; Maccioni et al., 2010; Craig et al., 2011; Karran et al., 2011; Checler and Turner, 2012; Alzheimer's Association, 2013; Kametani and Hasegawa, 2018). Several studies suggest the correlation of AD with AIS proteins and have shown the loss of AnkG and Na_v channels in AD brain samples (Kim et al., 2007; Sun et al., 2014). Cleavage of Na_v channel is associated with increase in

[1]Centre of Advanced Computational Solutions (C-fACS), Lincoln University, Christchurch, New Zealand; [2]Department of Molecular Biosciences, Lincoln University, Christchurch, New Zealand

***Correspondence to:** Don Kulasiri, PhD, Don.Kulasiri@lincoln.ac.nz.
https://orcid.org/0000-0001-8744-1578 (Don Kulasiri)

How to cite this article: *Bhardwaj P, Kulasiri D, Samarasinghe S (2021) Modeling protein-protein interactions in axon initial segment to understand their potential impact on action potential initiation. Neural Regen Res 16(4):700-706.*

Amyloid β peptides (Aβ) production, a protein responsible for the amyloid plaques in AD patients (Kim et al., 2007; Kovacs et al., 2010). Moreover, loss of AnkG from AIS structure could play a critical role in AD pathogenesis by disturbing the protein trafficking within the neuron by altering the function of molecular motors (Kinesin and Dynein) (Kim et al., 2007; Sun et al., 2014).

Biological systems are complex as their features can be explained using different methods, and this makes them very difficult to study and to predict their behaviors (Bailey et al., 2002). However, computational models can be used to understand the plausible molecular mechanisms in an organism at the molecular level if we carefully develop the questions to be investigated. As we mentioned before, AP initiation is associated with the high number of Na_v channels in the AIS, and these channels are phosphorylated by CK2 at their serine sites before their accumulation in the AIS. Further, AnkG recruits the phosphorylated Na_v channels in this region. The dynamics of the phosphorylated channels, CK2, and AnkG would have crucial effects on AP initiation, and any impairment of these interactions would perhaps explain the experimentally observed link of AnkG to AD pathogenesis. Hence, we develop a mathematical model to investigate the role of serine-specific phosphorylation of Na_v channels by CK2 before the accumulation of Na_v channels into the AIS. Also, we test the effect of changes in the initial concentration of CK2 and AnkG on the accumulation of Na_v channels at the AIS. Here, we suggest the AIS association with Alzheimer's disease (AD) pathogenesis by reporting CK2 mediated serine specific phosphorylation is necessary for the recruitment of Na_v channels into the AIS through AnkG. CK2 mediated phosphorylation increases the binding affinity with AnkG. Moreover, initial concentration of both AnkG and CK2 is also important and can disturb the final Na_v channel population in AIS. According to the literature, alteration in Na_v channels is associated with amyloid β peptides main component of amyloid plaques in AD patients (Kim et al., 2007; Kovacs et al., 2010).

Materials and Methods

Development of AIS models

It is necessary to make simplifying assumptions in the development of the model so that we can understand the interactions between the proteins within AIS. By using Virtual cell (version 7.2.0, Uconn Health, USA) software with currently available experimental data and insights (see References), the following assumptions are made:

1) The AIS region is considered as a cylinder with a length of 40 μm and a diameter of 1.5 μm (Gulledge and Bravo, 2016). A total of 12 species are present in our model which includes four different Na_v channels (NaA, NaB, NaC, and N_{1111}), four AnkG species (G1, G2, G3, and G4) and four CK2 species (C1, C2, C3, and C4).

2) In this model, four types of Na_v channels are considered based on different phosphorylation events within the channels. We assume five phosphorylation conditions: no site phosphorylation, single-site phosphorylation, double-site phosphorylation, triple-site phosphorylation and four-site phosphorylation (**Figure 3**). The no site phosphorylation means that all serine sites are in the non-phosphorylated state. We do not consider any Na_v species in this model as not being phosphorylated because without any serine phosphorylation, Na_v-AnkG interactions are impossible (Brechet et al., 2008). Similarly, none of the Na_v species are assumed to be in the single-site phosphorylation condition as well, because AnkG does not bind to the Na_v channels with single-site phosphorylation (Brachet et al., 2008). Four Na_v species in the model are assumed based on double-site phosphorylation, triple-site phosphorylation, and four-site phosphorylation. Due to the lack of literature on the concentration of Na_v channels before its restriction into the AIS, we estimate that the concentration of each of NaA, NaB, NaC, and N_{1111} as 3.32×10^{-12} μM.

3) The four phosphorylation sites in the AIS motifs (S1112, S1123, S1124 and S1126) are denoted by S1 = S1112, S2 = S1123, S3 = S1124, and S4 = S1126. All these sites within the Na_v channels are responsible for equally strong interactions between the Na_v channels and AnkG (Cantrell et al., 2018).

Here are the phosphorylation sequences for all four sites in the Na_v species:

• The phosphorylation of S1 is the first preference for CK2 because the regions near S1 (E, S1, D, F, and E) fulfill the criteria for the minimum consensus sequence (S/T, X, X, and D/E/pS/pT) for CK2 phosphorylation (**Figure 4**). The presence of acidic residues at the $n + 1$ and $n + 3$ positions makes S1 the most suitable site for phosphorylation by CK2 (Meggio and Pinna, 2003).

• S3 also fulfills the minimum criterion for the consensus sequence (S/T, X, X, and D/E/pS/pT). S3 also has acidic residues at the $n + 1$ and $n + 3$ positions, similar to S1 (**Figure 4**). However, S3 is assumed to be the second preference after S1 because S1 is located near the N-terminal.

• S4 is considered the third phosphorylation site because of the presence of an acidic residue (D) at the $n + 1$ position (**Figure 4**). The fourth, and final, phosphorylation site is S2 (S2, pS, E, pS, and D) because the region near S2 fulfills the minimum consensus sequence due to the presence of phosphorylated S or T at the $n + 1$ and $n + 3$ positions (**Figure 4**).

4) Phosphorylation of the Na_v species (NaA, NaB, NaC, and N_{1111}) by CK2 (C1, C2, C3, and C4) and its interaction with AnkG (G1, G2, G3, and G4) in this model are based on the mass action law.

5) In general, the phosphorylation is modeled using Michael-Menten kinetics (Wang and Wu, 2002) but due to rapid binding and unbinding of CK2 to the sites, we assume that the binding-unbinding can be modeled as elementary reactions and follows the mass action kinetics within the first few minutes; i.e., the serine related phosphorylation of Na_v channels by CK2 is considered as a reversible elementary reaction. Because of the importance of the serine residues, the main aim is to understand the binding of CK2 with the Na_v channels. Protein kinases have significant effects on the target protein they bind to. Protein kinases go on and off by auto-phosphorylation by binding with inhibitors or activator proteins or other small molecules. Their activity is highly regulated. However, this is not the case with CK2 due to its pleiotropic nature: CK2 does not require any mediators to activate because CK2 is always active. There is no evidence in the literature for any regulation of CK2 activity. CK2 not only phosphorylates the Na_v and Kv channels but also AnkG. Another reason for considering the mass action law to model the phosphorylation of Na_v species (NaA, NaB, NaC, and N_{1111}) is the abundance of CK2 in the brain; therefore, we assume negligible competition of other species for CK2. In the absence of data, the phosphorylation of all four Na_v species is assumed to occur at the same association (K_{on}) and dissociation rates (K_{off}).

6) In the brain, more than 300 substrates are available for CK2-mediated phosphorylation (Meggio and Pinna, 2003; Nishi et al., 2014). We have no data on the exact number of CK2 molecules required for phosphorylation of the Na_v channels. As CK2 present in abundance, we assume that the total CK2 concentration is 5.28×10^{-8} (μM). Specifically, for this model, total CK2 concentration is divided into four equal concentrations designated as C1, C2, C3, and C4 to phosphorylate NaA, NaB, NaC, and N_{1111}, respectively.

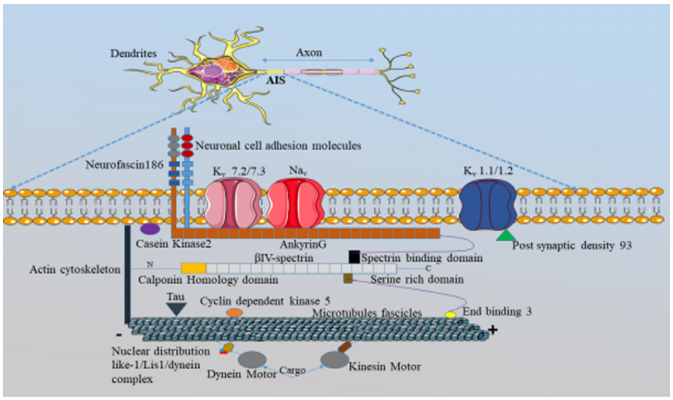

Figure 1 | A schematic diagram of the AIS structure.
The AIS region of neurons consists of three membranes: the plasma membrane, the spectrin-actin membrane, and the microtubule related membrane. Each membrane carries out different functions that favor AP initiation at the AIS. AnkG acts as the master organizer and all the proteins in the AIS are directly or indirectly associated with it (Zhang and Bennet, 1998; Zhou et al., 1998; Hedstrom et al., 2008; Cunha and Mohler, 2009; Nelson and Jenkins, 2017). The initial part of AnkG is called the membrane-binding domain, to which the anchoring of Na_v, and K_v channels (K_v 7.2/7.3) occurs (Nelson and Jenkins, 2017; Buffington and Rasband, 2011). At the AIS, the proteins binding with AnkG have specific amino acid sequence, known as the AIS motif, except for the K_v 1.1/1.2 channels (Schafer et al., 2009). Instead of AnkG, the recruitment of K_v 1.1/1.2 channels into the AIS depends on the post-synaptic density 93 (PSD 93) protein (Leterrier and Dargent, 2014; Yoshimura and Rasband, 2014). The membrane-binding domain is followed by a spectrin binding domain in the AnkG structure, and this is responsible for the binding between β-IV spectrin and AnkG (Jones and Svitkina, 2016). The microtubule fascicles in the AIS are also restricted by AnkG due to the interactions with an end binding 3 (EB3) protein (Nakata and Hirokawa, 2003; Jones and Svitkina, 2016). According to the experimental evidence, the high-density presence of Na_v channels in the AIS is correlated to the AP initiation (Kole et al., 2012; Jones and Svitkina, 2016); and it depends not only on AnkG but also on casein kinase 2 (CK2)-facilitated phosphorylation (Brechet et al., 2008). The experimental investigations have also shown that CK2 plays a dynamic role in the AIS region, especially in the accumulation of Na_v channels into the AIS (Brechet et al., 2008; Nishi et al., 2014; Xu and Cooper, 2015). AIS: Axon initial segment; AnkG: ankyrin-G; AP: action potential; K_v: voltage-gated potassium channel; MT: microtubule; Na_v: voltage-gated sodium channel; NF186: neurofascin 186; NrCAM: neuronal cell adhesion molecule.

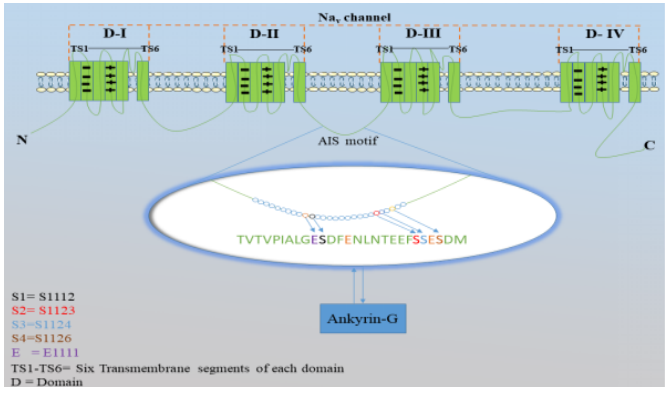

Figure 2 | A schematic representation of the AIS motif within Na_v channels.
The Na_v channels comprise of four domains (D-I–IV), and each domain contains six transmembrane segments (TS1–TS6). The AIS motif (enlarged area) is located between the II and III domains of the Na_v channels, and is made up of different 27 amino acids, with three main ones: serine (S) at the positions 1112, 1123, 1124, and 1126; glutamate (E) at the positions 1111 and 1115; and aspartate (D) at the position, 1113. Serine is important because the phosphorylation of Na_v channels is accomplished by CK2, and CK2 is specific for serine or threonine. The presence of negative residues, such as glutamate and aspartate is also significant because they provide the support for the CK2-mediated phosphorylation of serine. Moreover, glutamate and aspartate assist CK2 in the identification of serine as a target for phosphorylation. This figure was produced using Servier Medical Art (https://smart.servier.com). AIS: Axon initial segment; AnkG: ankyrin-G; Na_v: voltage-gated sodium channel.

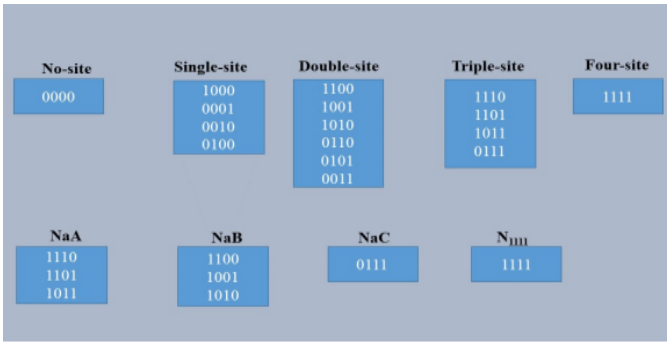

Figure 3 | Classification of the Na_v species in the AIS model.
None of the Na_v species in the model is in the no phosphorylation or single-site phosphorylation conditions. In the double-site phosphorylation, two serine sites are phosphorylated, and there is a total of six combinations. Out of the six, only the first three combinations are considered for Na_v-AnkG binding. These three combinations are considered as one and called NaB in the model. Combinations in the double phosphorylation condition, other than first three (NaB), are ignored based on the absence of an S1 site because the affinity of Na_v channel binding with AnkG is high in the presence of the S1 site (Fache et al., 2004; Brechet et al., 2008). In the triple-site phosphorylation conditions, all combinations favor the interaction of Na_v-AnkG. We, therefore, consider these first three combinations because of the presence of S1 and assume them as another Na_v species (NaA) in the model; the fourth combination of the triple phosphorylation condition is taken as the third Na_v species (NaC) even in the absence of an S1 site because of the phosphorylation of the remaining three serine sites (S2, S3, and S4) can favor Na_v-AnkG interactions but with a low binding affinity (Brechet et al., 2008). The fourth Na_v species (N_{1111}) in the model is based on the presence of all serine sites being in the phosphorylated state.

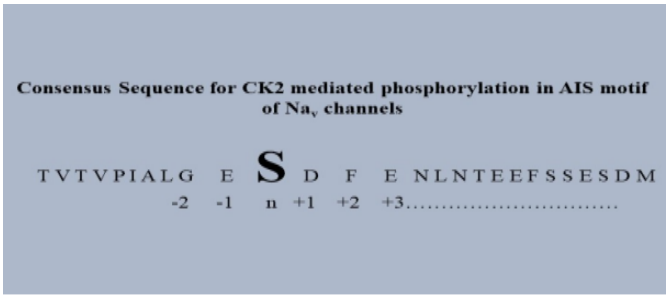

Figure 4 | Consensus sequence for CK2 mediated phosphorylation.
The AIS motif of Na_v channels and the requirements for CK2-mediated phosphorylation. S represents serine residues; E refers to glutamate, and D refers to aspartate. D and E assist CK2 to find suitable serine for phosphorylation (Meggio and Pinna, 2003; Nishi et al., 2014). The positions of residues within the motif are represented by $n-1$, n, $n+1$, and so on. The potential targets of CK2 for phosphorylation are serine/threonine residues in a motif surrounded by any of the acidic residues, such as E and D. CK2-mediated phosphorylation of serine/threonine requires at least one acidic residue between the $n-4$ to $n+7$ positions (Meggio and Pinna, 2003; Nishi et al., 2014). The most favorable serine for CK2-mediated phosphorylation is when an acidic residue is present at the $n+3$ position within a motif. In some instances, the phosphorylation by CK2 is enabled when an acidic residue is present at the $n+1$ position and this is the second most preferred position after $n+3$ (Meggio and Pinna, 2003; Nishi et al., 2014). The minimum consensus sequence for CK2 phosphorylation is S/T, X, X, D/E/pS/pT, where S/T is a serine or threonine in the n^{th} position, followed by any type residue at the $n+1$ and $n+2$ positions. At the $n+3$ position, D/E/pS/pT stands for aspartate (D) or glutamate (E) or phosphorylated serine/threonine (pS/ pT), respectively. Phosphorylated serine or threonine mimics the function of acidic residues and makes serine/threonine at the n position suitable for CK2 phosphorylation. The presence of basic residues (lysine, proline, and lysine) at the $n+1$, $n+2$, or $n+3$ positions has a negative impact on CK2-mediated phosphorylation. In this figure, the presence of a negative residue (E) at $n+3$ in the sequence makes S at the nth position suitable for phosphorylation by CK2 (Fache et al., 2004). S at the n^{th} position is phosphorylated first because it is near the N-terminal when compared to the other serine residues. Similarly, other serine residues in the AIS motif can be identified as targets for CK2 by assuming them at n positions and by checking nearby for the presence of negative residues (D/E/pS/pT). AIS: Axon initial segment; CK2: casein kinase 2; Na_v: voltage-gated sodium channel.

7) According to the literature, the total number of Na_v channels present in the AIS after binding with AnkG is 100–300 molecules/μm (Kole and Stuart, 2012). On the other hand, according to Srinivasan et al. (1988), AnkG numbers are ten times higher than the Na_v channels (Srinivasan et al., 1988). Based on this observation, in this model initial AnkG concentration is assumed as 1.32×10^{-13} μM. Similar to CK2 species, for this model, we divide AnkG species into four species named as G1, G2, G3 and G4 with the equal concentration of 3.32×10^{-14} μM; G1, G2, G3, and G4 bind with the phosphorylated form of NaA, NaB, NaC, and N_{1111}, respectively.

Equations in the AIS model

The schematic of the model is shown in **Figure 5**. All parameters in the model, including their initial concentrations and rate constants, were estimated in accordance with the literature (Srinivasan et al., 1988; Meggio and Pinna, 2003; Ubersax and Ferrell, 2007; Brechet et al., 2008; Kole et al., 2008; **Tables 1** and **2**).

Phosphorylation of Na_v species by CK2

Equations 1 to 20 models the dynamic changes in all Na_v species (NaA, NaB, NaC and N1111) after phosphorylation mediated by CK2 (C1, C2, C3, and C4) based on ordinary differential equations. The phosphorylated forms of the Na_v species are denoted as *pNaA*, *pNaB*, *pNaC* and pN_{1111}. [*NaA*], [*NaB*], [*NaC*], [N_{1111}], [*pNaA*], [*pNaB*], [*pNaC*], [pN_{1111}], [*C1*], [*C2*], [*C3*] and [*C4*]represent the concentration of the species. The phosphorylation of all Na_v species by CK2 species in Equation (1), (6), (11), and (16) are achieved at specific association rates (K_{01}, K_{02}, K_{03} and K_{04}) and dissociation rates (K_{10}, K_{20}, K_{30} and K_{40}).

$$NaA + C1 \underset{K_{10}}{\overset{K_{01}}{\longleftrightarrow}} pNaA \quad (1)$$

$$d[NaA]/dt = -K_{01}[NaA][C1] + K_{10}[pNaA] \quad (2)$$

$$d[C1]/dt = -K_{01}[NaA][C1] + K_{10}[pNaA] \quad (3)$$

$$d[pNaA]/dt = K_{01}[NaA][C1] - K_{10}[pNaA] \quad (4)$$

$$d[NaA]/dt = d[C1]/dt = -\{d[pNaA]/dt\} \quad (5)$$

$$NaB + C2 \underset{K_{20}}{\overset{K_{02}}{\longleftrightarrow}} pNaB \quad (6)$$

$$d[NaB]/dt = -K_{02}[NaB][C2] + K_{20}[pNaB] \quad (7)$$

$$d[C2]/dt = -K_{02}[NaB][C2] + K_{20}[pNaB] \quad (8)$$

$$d[pNaB]/dt = K_{02}[NaB][C2] - K_{20}[pNaB] \quad (9)$$

$$d[NaB]/dt = d[C2]/dt = -\{d[pNaB]/dt\} \quad (10)$$

$$NaC + C3 \underset{K_{30}}{\overset{K_{03}}{\longleftrightarrow}} pNaC \quad (11)$$

$$d[NaC]/dt = -K_{03}[NaC][C3] + K_{30}[pNaC] \quad (12)$$

$$d[C3]/dt = -K_{03}[NaC][C3] + K_{30}[pNaC] \quad (13)$$

$$d[pNaC]/dt = K_{03}[NaC][C3] - K_{30}[pNaC] \quad (14)$$

$$d[NaC]/dt = d[C3]/dt = -\{d[NaC]/dt\} \quad (15)$$

$$N_{1111} + C4 \underset{K_{40}}{\overset{K_{04}}{\longleftrightarrow}} pN_{1111} \quad (16)$$

$$d[N_{1111}]/dt = -K_{04}[N_{1111}]\,[C4] + K_{40}[pN_{1111}] \quad (17)$$

$$d[C4]/dt = -K_{04}[N_{1111}]\,[C4] + K_{40}[pN_{1111}] \quad (18)$$

$$d[pN_{1111}]/dt = K_{04}[N_{1111}]\,[C4] - K_{40}[pN_{1111}] \quad (19)$$

$$d[N_{1111}]/dt = d[C4]/dt = -\{d[pN_{1111}]/dt\} \quad (20)$$

Binding of phosphorylated Na_v species with AnkG

Equations 21 to 40 describe the accumulation of Na_v species at the AIS after binding with AnkG. The ordinary differential equations for binding between the phosphorylated form of Na_v species (*pNaA*, *pNaB*, *pNaC* and pN_{1111}) and AnkG (G1, G2, G3, G4) are written using the mass action law. [*pNaA*], [*pNaB*], [*pNaC*], [pN_{1111}], [*pNaA* × *G1*], [*pNaB* × *G2*], [*pNaC* × *G3*], [pN_{1111} × *G4*], [*G1*], [*G2*], [*G3*] and [*G4*] represent the concentrations of the species. The binding of phosphorylated Na_v species with AnkG species in equations 21, 26, 31 and 36 is accomplished through the association rates (K_{05}, K_{06}, K_{07} and K_{08}) and the dissociation rates (K_{50}, K_{60}, K_{70} and K_{80}).

$$pNaA + G1 \underset{K_{50}}{\overset{K_{05}}{\longleftrightarrow}} pNaA \times G1 \quad (21)$$

$$d[pNaA]/dt = -K_{05}[pNaA][G1] + K_{50}[pNaA \times G1] \quad (22)$$

$$d[G1]/dt = -K_{05}[pNaA][G1] + K_{50}[pNaA \times G1] \quad (23)$$

$$d[pNaA \times G1]/dt = K_{05}[pNaA][G1] - K_{50}[pNaA \times G1] \quad (24)$$

$$d[pNaA]/dt = d[G1]/dt = -\{d[pNaA \times G1]/dt\} \quad (25)$$

$$pNaB + G2 \underset{K_{60}}{\overset{K_{06}}{\longleftrightarrow}} pNaB \times G2 \quad (26)$$

$$d[pNaB]/dt = -K_{06}[pNaB][G2] + K_{60}[pNaB \times G2] \quad (27)$$

$$d[G2]/dt = -K_{06}[pNaB][G2] + K_{60}[pNaB \times G2] \quad (28)$$

$$d[pNaB \times G2]/dt = K_{06}[pNaB][G2] - K_{60}[pNaB \times G2] \quad (29)$$

$$d[pNaB]/dt = d[G2]/dt = -\{d[pNaB \times G2]/dt\} \quad (30)$$

$$pNaC + G3 \underset{K_{70}}{\overset{K_{07}}{\longleftrightarrow}} pNaC \times G3 \quad (31)$$

$$d[pNaC]/dt = -K_{07}[pNaC][G3] + K_{70}[pNaC \times G3] \quad (32)$$

$$d[G3]/dt = -K_{07}[pNaC][G3] + K_{70}[pNaC \times G3] \quad (33)$$

$$d[pNaC \times G3]/dt = K_{07}[pNaC][G3] - K_{70}[pNaC \times G3] \quad (34)$$

$$d[pNaC]/dt = d[G3]/dt = -\{d[pNaC \times G3]/dt\} \quad (35)$$

$$pN_{1111} + G4 \underset{K_{80}}{\overset{K_{08}}{\longleftrightarrow}} pN_{1111} \times G4 \quad (36)$$

$$d[pN_{1111}]/dt = -K_{08}[pN_{1111}]\,[G4] + K_{80}[pN_{1111} \times G4] \quad (37)$$

$$d[G4]/dt = -K_{08}[pN_{1111}]\,[G4] + K_{80}[pN_{1111} \times G4] \quad (38)$$

$$d[pN_{1111} \times G4]/dt = K_{08}[pN_{1111}][G4] - K_{80}[pN_{1111} \times G4] \quad (39)$$

$$d[pN_{1111}]/dt = d[G4]/dt = -\{d[pN_{1111} \times G4]/dt\} \quad (40)$$

Results

Using the computational model, we tested the role of serine site in the recruitment of Na_v channels into the AIS to understand the nature of binding of all phosphorylated Na_v species (NaA, NaB, NaC, and N_{1111}) with AnkG species (G1, G2, G3, and G4) (**Figure 6**). The binding of pN_{1111} with G4 and achieves the highest concentration of the pN_{1111} recruited by

Table 1 | Initial concentration of all species considered in the axon initial segment model

Protein	Initial concentration (μM)	Source
NaA	3.32×10^{-12}	Kole et al. (2008)
NaB	3.32×10^{-12}	Kole et al. (2008)
NaC	3.32×10^{-12}	Kole et al. (2008)
N1111	3.32×10^{-12}	Kole et al. (2008)
C1	1.32×10^{-8}	Meggio and Pinna (2003)
C2	1.32×10^{-8}	Meggio and Pinna (2003)
C3	1.32×10^{-8}	Meggio and Pinna (2003)
C4	1.32×10^{-8}	Meggio and Pinna (2003)
G1	3.32×10^{-14}	Srinivasan et al. (1988)
G2	3.32×10^{-14}	Srinivasan et al. (1988)
G3	3.32×10^{-14}	Srinivasan et al. (1988)
G4	3.32×10^{-14}	Srinivasan et al. (1988)

G4 (2.64×10^{-15} μM or equivalent to 1565 molecules within the AIS volume) among all Na_v species. These results are supported by the study in which 100–300 Na_v molecules/μm of the AIS are documented (Kole et al., 2008). The higher concentration of pN_{1111} after binding to G4 indicates that in the presence of all serine sites, the binding with AnkG takes place with a strong binding affinity, which corroborated with the experimental evidence (Fache et al., 2004; Brechet et al., 2008). This strong binding affinity is responsible for the high density of Na_v channels at the AIS. Na_v species other than pN_{1111} shows a dramatic decrease in their protein concentrations after binding with AnkG. After binding with G1, pNaA species has the second-highest concentration (7.2×10^{-16} μM or equivalent to 433 molecules within the AIS volume). As mentioned in the assumptions, the fact that pNaA consists of three serine sites including S1 could be the reason for this significant reduction of pNaA as compared to pN_{1111}. Remaining Na_v species (pNaB and pNaC) after their respective binding with G2 and G3 show almost similar concentration but lesser than pN_{1111} and pNaA (3.8×10^{-16} μM or equivalent to 205 molecules in the AIS volume, and 3.8×10^{-16} μM or equivalent to 228 molecules in the AIS volume) respectively. Similar concentrations of pNaB and pNaC after binding with AnkG species demonstrate the importance of the S1 site in the AIS motif. Similar results are given by Brechet et al. (2008), where the concentration of the Na_v channels after S1 mutation is the same as the Na_v channels with a double site mutation in the presence of S1 (Brechet et al., 2008). The S1 site within the AIS motif of a Na_v channel is surrounded by acidic residues, such as glutamate and aspartate. The presence of these acidic residues increases the importance of the S1 site by increasing its probability of being phosphorylated by CK2 as the first preference. This could be the reason for pNaB to show a similar behavior compared to the pNaC species (S1 absence).

Therefore, the availability of all serine sites for CK2-mediated phosphorylation is necessary for the regulation of the Na_v channel population at the AIS to maintain the conditions suitable for AP initiation. Besides, any alteration in the phosphorylation conditions can cause a disturbance in the recruitment of Na_v into the AIS by preventing Na_v-AnkG binding. According to the literature, any alteration in the Na_v channel densities at the AIS can increase the threshold voltage required for AP initiation. This disturbance in the AIS system can shift the AP initiation zone from AIS to a region such as the nodes of Ranvier with a high number of Na_v channels after AIS (Lemaillet et al., 2003; Kole et al., 2008; Rasband, 2009; Gulledge and Bravo, 2016; Satake et al., 2017). However, NOR, as an AP initiator zone, cannot hold the voltage stress during AP due to its position away from the soma (Kole et al., 2008, 2012).

Table 2 | Rate constants used in the axon initial segment model with their biological meaning

Rate constants	Biological meaning	Values	Source
K_{01}	Association rate for NaA and C1	1×10^{12} (μM/s)	Ubersax and Ferrell (2007)
K_{10}	The dissociation rate of pNaA into NaA and C12	1×10^{6} (/s)	Ubersax and Ferrell (2007)
K_{02}	Association rate for NaB and C2	1×10^{12} (μM/s)	Ubersax and Ferrell (2007)
K_{20}	The dissociation rate of pNaB into NaB and C2	1×10^{6} (/s)	Ubersax and Ferrell (2007)
K_{03}	Association rate for NaC and C3	1×10^{12} (μM/s)	Ubersax and Ferrell (2007)
K_{30}	The dissociation rate of pNaC into NaC and C3	1×10^{6} (/s)	Ubersax and Ferrell (2007)
K_{04}	Association rate of N_{1111} and C4	1×10^{12} (μM/s)	Ubersax and Ferrell (2007)
K_{40}	The dissociation rate of pN_{1111} into N_{1111} and C4	1×10^{6} (/s)	Ubersax and Ferrell (2007)
K_{05}	Association rate of pNaA and G1	1.71×10^{9} (μM/s)	Brechet et al. (2008)
K_{50}	The dissociation rate of pNaA × G1 into pNaA and G1	3.3×10^{-3} (/s)	Brechet et al. (2008)
K_{06}	Association rate of pNaB and G2	$8.2 \pm 2.6 \times 10^{8}$ (μM/s)	Brechet et al. (2008)
K_{60}	Dissociation rate of pNaB × G2 into pNaB and G2	$3.4 \pm 0.2 \times 10^{-3}$ (/s)	Brechet et al. (2008)
K_{07}	Association rate of pNaC and G3	$8.9 \pm 0.2 \times 10^{8}$ (μM/s)	Brechet et al. (2008)
K_{70}	The dissociation rate of pNaC × G3 into pNaC and G3	$3.3 \pm 0.4 \times 10^{-3}$ (/s)	Brechet et al. (2008)
K_{08}	Association rate of pN_{1111} and G4	4.24×10^{9} (μM/s)	Brechet et al. (2008)
K_{80}	The dissociation rate of pN_{1111} × G4 into pN_{1111} and G4	$2.1 \pm 0.8 \times 10^{-3}$ (/s)	Brechet et al. (2008)

Effect of change in the initial concentrations of CK2 on Na_v channel recruitment at AIS

To test the significance of the initial concentration of CK2 on the Na_v channel recruitment at AIS, we phosphorylated N_{1111} species at ten different CK2 (C2) initial concentrations and observed its impact on the binding of pN_{1111} with AnkG (G4) (**Figure 7**). The initial concentration of C2 was taken within a range of 6.6×10^{-9} μM to 1.98×10^{-8} μM. According to the results, at low initial C2 concentration (6.6×10^{-9} μM), lesser pN_{1111} molecules bound to G4 (1.38×10^{-15} μM or equivalent to 833 molecules in the AIS volume). As we increased the initial C2 concentration, pN_{1111} molecules were also increased after binding with G4. These results indicate the dependency of binding affinity between Na_v channels and AnkG on the CK2 concentration. Similar results were reported by various studies that supported the importance of CK2 (Brechet et al., 2008; Hsu et al., 2017). Hsu et al. (2017) showed that the inhibition of CK2 using 4,5,6,7-tetrabromobenzotriazole significantly altered the binding of Na_v channels with AnkG by eliminating their CK2-mediated phosphorylation. In addition to that, CK2 inhibition shortened the axons by 30% (Ponce et al., 2011). Our model and the experimental studies so far show that CK2 plays a critical role in the AIS by enhancing the binding affinity between Na_v channels and AnkG (Brechet et al., 2008; Ponce et al., 2011; Hsu et al., 2017).

Effects of the initial concentrations of AnkG on Na_v channel recruitment at AIS

To test the role of AnkG, we introduced ten new initial concentrations of G4 in the present model. The concentration range of G4 was set to from 1.66×10^{-14} to 4.98×10^{-14} μM. Binding of G4 with pN_{1111} was taken into account to test the impact of AnkG on the binding of Na_v channels into the AIS. According to the results (**Figure 8**), at the low initial

concentration of G4, pN_{1111} levels were lower after binding with G4 (1.36×10^{-15} μM ~806 molecules of pN_{1111} in the AIS). However, as we increased the G4 initial concentration, the concentration of pN_{1111} after binding with G4 increased. At the highest initial concentration of G4, pN_{1111} achieved the highest value after binding with G4 (3.96×10^{14} μM /2394 molecules).

The population of the Na_v channels in the AIS region is higher than those in the soma region (Rasband, 2010). The high number of Na_v channels in the AIS region is reported by Kole et al. (2008); their experimental results suggest that the density of Na_v channels in this region is higher by 50-fold than that in the soma (Kole et al., 2008). The high number of Na_v channels in the structure of the AIS supports the AIS skeleton in overcoming the load-induced during AP initiation. Moreover, due to their high number, Na_v channels in the AIS region activate and deactivate much faster than the Na_v channels present in the soma. Also, the voltage required to change the membrane potential in AIS is low compared with the soma (Ogawa and Rasband 2008; Yoshimura and Rasband, 2014). However, the functions of AnkG are not limited by Na_v channel recruitment because, according to previous studies, AnkG is responsible for the recruitment of ion channels (Na_v and K_v), molecular motors (kinesin and dynein) and CAMs (NF186 and NrCAM) into the AIS (Zhang and Bennet, 1998; Zhou et al., 1998; Hedstrom et al., 2008; Cunha and Mohler, 2009; Nelson and Jenkins, 2017). Moreover, the function of AnkG is also related to protein trafficking within the neurons because AnkG is connected with microtubules through the EB3 protein. While the kinesin and dynein motors travel through microtubules to facilitate the proper trafficking of the proteins, AnkG related mutations can cause disturbances in the transportation of the proteins within neurons (Sun et al., 2014). Moreover, dendritic proteins, such as integrin-β1 and microtubule associated protein-2, have been found in the axons after AnkG mutation indicating an alteration in protein trafficking (Hedstorm et al., 2008).

Possible role of AIS in AD pathogenesis

The AIS mutations are not only restricted to the reduced ability of a neuron to generate action potential but also are associated with the development of seizures and epilepsy (Hauser et al., 1986). The role of AIS in AD pathogenesis has been studied. Experimental evidence showed that patients with sporadic AD have the risk of developing seizures especially after the onset of dementia (Hauser et al., 1986). On the other hand, the studies using AD brain samples found the presence of disturbed Na_v channels (Kim et al., 2007). Disturbed level of Na_v channels has potentially been associated with elevated BACE-1 (β-site amyloid precursor protein (APP) cleavage enzyme-1). Increased BACE-1 possibly inhibits the trafficking of channels to the AIS by preventing the molecular motors to perform their functions (Kim et al., 2007). The increased level of BACE-1 precipitated in AD pathogenesis by increasing pathogenic Aβ production and is associated with the cleavage of Na_v channel subunits (Kim et al., 2007; Kovacs et al., 2010). In mouse models of AD, the area around Aβ plaques showed synaptic losses, axonal swelling, and mutations in the neuronal network (Marin et al., 2016). Aβ plaques could cause damage near or around the region of AIS by targeting AnkG and βIV spectrin and decreasing the density and length of the AIS (Marin et al., 2016; Sohn et al., 2016). Disturbance in the AIS functions could be a consequence of the calpain-mediated proteolysis of AnkG and βIV spectrin due to the induction of Aβ (Buffington and Rasband, 2011; Marin et al., 2016). The low AnkG concentration can dismantle the structure of AIS by loosening the proteins anchored by AnkG. Dismantling the structure results in the disruption of neuronal polarity by abolishing the functions of the important proteins present in this region (Buffington and Rasband, 2011). The results are shown by Sun et al. (2014) support the relationship between AIS and AD by observing the low level of AnkG in AD transgenic mice. The lower level of AnkG could results in the alteration of Na_v channel at the AIS.

Conclusion

The importance of the serine sites (S1, S2, S3, and S4) in the accumulation of Na_v channels into the AIS to create suitable conditions for AP initiation has been shown through this modeling study which corroborates with the experimental findings. The results suggest that, in the presence of all the serine sites in Na_v channels for CK2-mediated phosphorylation, the binding between the Na_v channels and AnkG takes place with a strong binding affinity. We showed the significance of the initial concentrations of CK2 and AnkG on the recruitment of Na_v channels. From the simulation results, we observed that the low initial levels of CK2 and AnkG reduced the population of the Na_v channels at the AIS. At low levels of CK2, the Na_v channels are not fully phosphorylated, which weakens the binding between the Na_v channels and AnkG. Moreover, at low AnkG concentration, the AIS structural assembly dismantles which could create difficulties in the proper trafficking of proteins into the AIS such as Na_v channels. Low levels of Na_v channels increase the voltage required to initiate AP. Overall, these results indicate the potentially strong association of AIS proteins in AD pathogenesis. Future experimental investigation into the activity levels of AIS related CK2 in AD brains may shed light into the more confirmed role of CK2 in AD pathogenesis.

Author contributions: *DK conceptualized and led the project. PB developed the model with DK. DK and SS supervised the project. PB and DK wrote the paper. SS independently critiqued the first draft. All authors approved the final version of the paper.*
Conflicts of interest: *There are no competing interests .*
Financial support: *None.*
Institutional review board statement: *Ethical issues are not needed to be considered in undertaking this study.*

Data sharing statement: *Datasets analyzed during the current study are available from the corresponding author on reasonable request.*
Plagiarism check: *Checked twice by iThenticate.*
Peer review: *Externally peer reviewed.*

References

Alzheimer's Association (2013) 2013 Alzheimer's disease facts and figures. Alzheimer's Dement 9:208-245.
Baley C, Lu H, Glinski G, Wheeler D, Hamilton P, Hendriksen M, Smith B (2002) Using computer models to identify optimal conditions for flip-chip assembly and reliability. Circuit World 28:14-20.
Bi C, Wu J, Jiang T, Liu Q, Cai W, Yu P, Cai T, Zhao M, JiangY H, Sun ZS (2012) Mutations of ANK3 identified by exome sequencing are associated with autism susceptibility. Hum Mutat 33:1635-1638.
Bian Y, Ye M, Wang C, Cheng K, Song C, Dong M, Pan Y, Qin H, Zou H (2013). Global screening of CK2 kinase substrates by an integrated phosphoproteomics workflow. Sci Rep 3:1-7.
Bréchet A, Fache MP, Brachet A, Ferracci G, Baude A, Irondelle M, Pereira S, Leterrier C, Dargent B (2008) Protein kinase CK2 contributes to the organization of sodium channels in axonal membranes by regulating their interactions with ankyrin G. J Cell Biol 183:1101-1114.
Buffington SA, Rasband MN (2011) The axon initial segment in nervous system disease and injury. Eur J Neurosci 34:1609-1619.
Cantrell AR, Scheuer T, Catterall WA (2018) Voltage-dependent neuromodulation of Na+ channels by D1-like dopamine receptors in rat hippocampal neurons. J Neurosci 19:5301-5310.
Checler F, Turner AJ (2012) Journal of Neurochemistry Special Issue on Alzheimer's Disease: Amyloid cascade hypothesis- 20 years on'. J Neurochem 120 Suppl 1:iii-iv.
Craig LA, Hong NS, McDonald RJ (2011) Revisiting the cholinergic hypothesis in the development of Alzheimer's disease. Neurosci Biobehav Rev 35:1397-1409.
Cunha SR, Mohler PJ (2009) Ankyrin protein networks in membrane formation and stabilization. J Cell Mol Med 13(11-12):4364-4376.
Fache MP, Moussif A, Fernandes F, Giraud P, Garrido J, Dargent B (2004) Endocytotic elimination and domain-selective tethering constitute a potential mechanism of protein segregation at the axonal initial segment. J Cell Biol 166:571-578.
Fan X, Markram H (2019) A brief history of simulation neuroscience. Front Neuroinform 13:32.
Gulledge AT, Bravo JJ (2016) Neuron morphology influences axon initial segment plasticity. eNeuro 3. pii: ENEURO.0085-15.2016.
Hardy J, Higgins G (1992) Alzheimer's disease: the amyloid cascade hypothesis. Science 256:184-185.
Harty RC, Kim TH, Thomas EA, Cardamone L, Jones NC, Petrou S, Wimmer VC (2013) Axon initial segment structural plasticity in animal models of genetic and acquired epilepsy. Epilepsy Res 105:272-279.
Hedstrom KL, Ogawa Y, Rasband MN (2008) AnkyrinG is required for maintenance of the axon initial segment and neuronal polarity. J Cell Biol 183:635-640.
Hsu WJ, Wildburger NC, Haidacher SJ, Nenov MN, Folorunso O, Singh AK, Chesson BC, Franklin WF, Cortez I, Sadygov RG, Dineley KT, Rudra JS, Taglialatela G, Lichti CF, Denner L, Laezza F (2017) PPARgamma agonists rescue increased phosphorylation of FGF14 at S226 in the Tg2576 mouse model of Alzheimer's disease. Exp Neurol 295:1-17.
Jones SL, Svitkina TM (2016) Axon initial segment cytoskeleton: architecture, development, and role in neuron polarity. Neural Plast 2016:6808293.
Kametani F, Hasegawa M (2018) Reconsideration of amyloid hypothesis and tau hypothesis in Alzheimer's disease. Front Neurosci 12:25.
Kaphzan H, Buffington SA, Jung JI, Rasband MN, Klann E (2011) Alterations in intrinsic membrane properties and the axon initial segment in a mouse model of angelman syndrome. J Neurosci 31:17637-17648.
Karran E, Mercken M, De Strooper B (2011) The amyloid cascade hypothesis for Alzheimer's disease: an appraisal for the development of therapeutics. Nat Rev Drug Discov 10:698-712.
Katsuki T, Ailani D, Hiramoto M, Hiromi Y (2009) Intra-axonal patterning: intrinsic compartmentalization of the axonal membrane in drosophila neurons. Neuron 64:188-199.

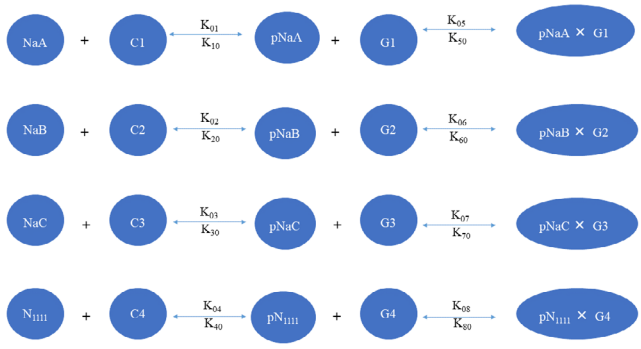

Figure 5 | Model for the accumulation of Na_v channels in the axon initial segment.
The model contains 12 different species: CK2 (C1, C2, C3, C4), Na_v (NaA, NaB, NaC, N_{1111}), and AnkG (G1, G2, G3, G4); and sixteen rate constants. A total of eight reactions are used to model the phosphorylation (p) of Na_v species through CK2 and the binding of phosphorylated Na_v species to AnkG. AnkG: ankyrin-G; CK2: casein kinase 2; Na_v: voltage-gated sodium channel.

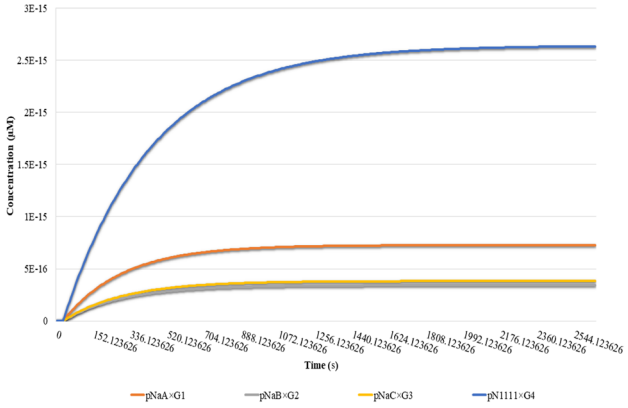

Figure 6 | Binding of Na_v species with AnkG species (G1, G2, G3, and G4) under different phosphorylation conditions.
The effect of the presence and absence of serine sites within Nav channels is shown. Time in seconds on *x*-axis explains the simulation time and *y*-axis describe the concentration Na_v channels (pNaA, pNaB, pNaC, and pN_{1111}) after binding with AnkG (G1, G2, G3, and G4). The blue line represents the highest concentration of pN_{1111} due to the presence of all four serine sites for casein kinase 2-mediated phosphorylation. The orange line denotes the effect of the absence of two serine residues on the pNaA concentration. The concentration of the remaining two phosphorylated Na_v species (pNaC and pNaB) are found to be at a similar level. However, their concentrations are lower than the concentrations of pN_{1111} and pNaA. AIS: Axon initial segment; AnkG: ankyrin-G; Na_v: voltage-gated sodium channel.

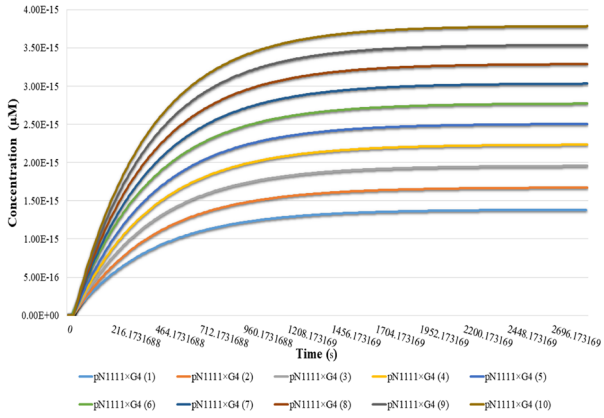

Figure 7 | Effect of initial concentrations of CK2 on the Na_v channels recruitment at AIS.
The effect of variation in initial CK2 concentration on the Na_v-AnkG binding is shown. Time in seconds on *x*-axis explains the simulation time in seconds and *y*-axis describe the concentration of pN_{1111} after binding with AnkG (G4). Binding between pN_{1111} and G4 is tested at ten different initial CK2 concentration. In figure pN_{1111} × G4(1) represents the binding of pN1111 with G4 at a low initial CK2 concentration (1) and pN_{1111}×G4 achieves the lowest concentration. However, as we increase the initial CK2 concentration, levels of pN_{1111}- G4 binding product also increase. AIS: Axon initial segment; AnkG: ankyrin-G; Na_v: voltage-gated sodium channel.

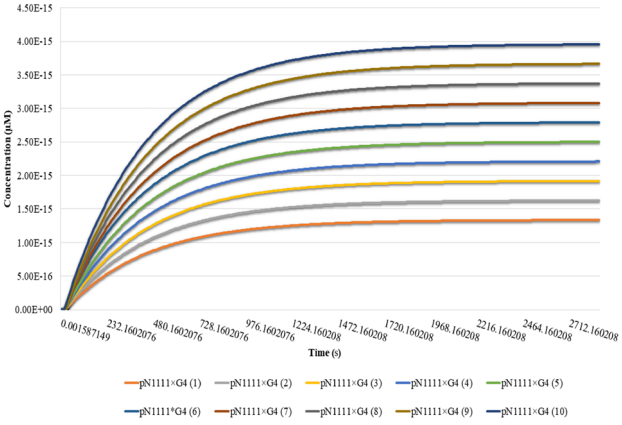

Figure 8 | Effect of different concentrations of AnkG on the Na_v channel recruitment at AIS.
The effect of variation in initial AnkG concentration on the Na_v-AnkG binding is shown. Time in seconds on x-axis explains the simulation time in seconds and y-axis describe the concentration of pN_{1111} after binding with AnkG (G4). Binding between pN_{1111}-G4 is tested at ten different AnkG initial concentrations. pN_{1111}×G4(1) represents the binding of pN_{1111} with G4 at the lowest initial AnkG concentration (1) and pN_{1111}×G4 binding achieved the lowest concentration. However, as we increase the initial AnkG concentration, levels of pN_{1111}- G4 binding product also increases. AIS: Axon initial segment; AnkG: ankyrin-G; Na_v: voltage-gated sodium channel.

Kim DY, Carey BW, Wang H, Ingano LA, Binshtok AM, Wertz MH, Pettingell WH, He P, Lee VM, Woolf CJ, Kovacs DM (2007) BACE1 regulates voltage-gated sodium channels and neuronal activity. Nat Cell Biol 9:755-764.
Kole MH, Ilschner SU, Kampa BM, Williams SR, Ruben PC, Stuart GJ (2008) Action potential generation requires a high sodium channel density in the axon initial segment. Nat Neurosci 11:178-186.
Kole MH, Stuart GJ (2012) Signal processing in the axon initial segment. Neuron 73:235-247.
Kovacs DM, Gersbacher MT, Kim D (2010) Alzheimer's secretases regulate voltage- gated sodium channels. Neurosci Lett 486:68-72.
Leterrier C, Dargent B (2014) No Pasaran! Role of the axon initial segment in the regulation of protein transport and the maintenance of axonal identity. Semin Cell Dev Biol 27:44–51.
Leterrier C, Potier J, Caillol G, Debarnot C, Rueda Boroni F, Dargent B (2015) Nanoscale architecture of the axon initial segment reveals an organized and robust scaffold. Cell Rep 13:2781-2793.
Maccioni RB, Farías G, Morales I, Navarrete L (2010) The revitalized tau hypothesis on Alzheimer's disease. Arch Med Res 41:226-231.
Marin MA, Ziburkus J, Jankowsky J, Rasband MN (2016) Amyloid-β plaques disrupt axon initial segments. Exp Neurol 281:93-98.
Meggio F, Pinna LA (2003) One-thousand-and-one substrates of protein kinase CK2. J FASEB 17:349-368.
Moraru II, Schaff JC, Slepchenko BM, Blinov ML, Morgan F, Lakshminarayana A, Gao F, Li Y, Loew LM (2008) Virtual Cell modelling and simulation software environment. IET Syst Biol 2:352-362.
Nakata T, Hirokawa N (2003) Microtubules provide directional cues for polarized axonal transport through interaction with kinesin motor head. J Cell Biol 162:1045-1055.
Nelson AD, Jenkins PM (2017) Axonal membranes and their domains: assembly and function of the axon initial segment and node of Ranvier. Front Cell Neurosci 11:1-17.
Nishi H, Shaytan A, Panchenko AR (2014) Physicochemical mechanisms of protein regulation by phosphorylation. Front Genet 5:1-10.
Peltola MA, Kuja-Panula J, Liuhanen J, Võikar V, Piepponen P, Hiekkalinna T, Taira T, Lauri SE, Suvisaari J, Kulesskaya N, Paunio T, Rauvala H (2016) AMIGO-Kv2.1 potassium channel complex is associated with schizophrenia-related phenotypes. Schizophr Bull 42:191-201.
Platkiewicz J, Brette R (2010) A threshold equation for action potential initiation. PLoS Comput Biol 6:e1000850.
Ponce D, Muñoz A, Garrido JJ (2011) Casein kinase 2 and microtubules control axon initial segment formation. Mol Cell Neurosci 46:222-234.
Rasband MN (2010) The axon initial segment and the maintenance of neuronal polarity. Nat Rev Neurosci 11:552-562.
Rasband MN (2008) Na+ channels get anchored...with a little help. J Cell Biol 183:975-977.
Rasband MN (2009) Converging on the origins of axonal ion channel clustering. PLoS Genet 5:e1000340.
Rueckert EH, Barker D, Ruderfer D, Bergen SE, O'Dushlaine C, Luce CJ, Sheridan SD, Theriault KM, Chambert K, Moran J, Purcell SM, Madison JM, Haggarty SJ, Sklar P (2013) Cis-acting regulation of brain-specific ANK3 gene expression by a genetic variant associated with bipolar disorder. Mol Psychiatry 18:922-929.
Schafer DP, Jha S, Liu F, Akella T, McCullough LD, Rasband MN (2009) Disruption of the axon initial segment cytoskeleton is a new mechanism for neuronal injury. J Neurosci 29:13242-13254.
Schmidt-Hieber C, Jonas P, Bischofberger J (2008) Action potential initiation and propagation in hippocampal mossy fibre axons. J Physiol 586:1849-1857.
Sohn PD, Tracy TE, Son HI, Zhou Y, Leite RE, Miller BL, Seeley WW, Grinberg LT, Gan L (2016) Acetylated tau destabilizes the cytoskeleton in the axon initial segment and is mislocalized to the somatodendritic compartment. Mol Neurodegener 11:47.
Srinivasan Y, Elmer L, Davis J, Bennett V, Angelides K (1988) Ankyrin and spectrin associate with voltage-dependent sodium channels in brain. Nature 333:177-180
Sun X, Wu Y, Gu M, Zhang Y (2014) MiR-342-5p decreases ankyrin G levels in Alzheimer's disease transgenic mouse models. Cell Rep 6:264-270.
Ubersax JA, Ferrell JE (2007) Mechanisms of specificity in protein phosphorylation. Nat Rev Mol Cell Biol 8:530-541.
Wang ZX, Wu JW (2002) Autophosphorylation of protein kinases. Biochem J 368:947-952
Xu M, Cooper E C (2015) An ankyrin-G N-terminal gate and protein kinase CK2 dually regulate binding of voltage-gated sodium and KCNQ2/3 potassium channels. J Biol Chem 290:16619-16632.
Yamada R, Kuba H (2016) Structural and functional plasticity at the axon initial segment. Front Cell Neurosci 10:250.
Yoshimura T, Rasband MN (2014) Axon initial segments: Diverse and dynamic neuronal compartments. Curr Opin Neurobiol 27:96-102.
Zhang X, Bennett V (1998) Restriction of 480/270-kD ankyrin G to axon proximal segments requires multiple ankyrin G-specific domains. J Cell Biol 142:1571-1581.

C-Editors: Zhao M, Li CH; T-Editor: Jia Y